SAND2014-0048C

Precision Laser Annealing of Silicon devices for Enhanced Electro-Optic Performance

Daniel A. Bender, Christopher T. DeRose, Andrew Starbuck, Jason C. Verley and Mark W. Jenkins

Sandia National Laboratories, PO Box 5800, Albuquerque, NM 87185, USA

ABSTRACT

We present results from laser annealing experiments in Si using a passively Q-switched Nd:YAG microlaser. Exposure with laser at fluence values above the damage threshold of commercially available photodiodes results in electrical damage (as measured by an increase in photodiode dark current). We show that increasing the laser fluence to values in excess of the damage threshold can result in annealing of a damage site and a reduction in detector dark current by as much as 100x in some cases. A still further increase in fluence results in irreparable damage. Thus we demonstrate the presence of a laser annealing window over which performance of damaged detectors can be at least partially reconstituted. Moreover dark current reduction is observed over the entire operating range of the diode indicating that device performance has been improved for all values of reverse bias voltage. Additionally, we will present results of laser annealing in Si waveguides. By exposing a small (<10 um) length of a Si waveguide to an annealing laser pulse, the longitudinal phase of light acquired in propagating through the waveguide can be modified with high precision, <15 milliradian per laser pulse. Phase tuning by 180 degrees is exhibited with multiple exposures to one arm of a Mach-Zehnder interferometer at fluence values below the morphological damage threshold of an etched Si waveguide. No reduction in optical transmission at 1550 nm was found after 220 annealing laser shots.

1. INTRODUCTION

Implementation of techniques to reduce dark current and noise on detectors offers potential deep impact to the quality of data gathered and processed by optical sensors and in particular focal plane arrays (FPAs). Ideally, such techniques would precisely target only pixels or clusters of pixels that are “hot” or noisy while leaving functional pixels untouched. Laser annealing provides a means to target problematic pixels delivering a localized amount of heat allowing them to reform under the conditions of a thermal anneal without affecting surrounding detector areas or readout circuitry.

Detectors of optical signals in the visible or infrared (IR) often undergo thermal annealing in manufacturing to allow dopant activation, thermal oxidation, metal reflow and chemical vapor deposition. Thermal annealing is typically done with equipment that heats the entire semiconductor wafer by using a lamp, hot plate or furnace. Lasers are also employed typically with a cylindrical lens focusing a beam into a line that is swept across the wafer, homogenizing the surface. The aim of this paper is to demonstrate laser annealing as an augmentation to thermal annealing on detectors after they have been hybridized with readout electronics and packaged or as a means of reconstituting lost detector capability from damaging laser exposure. For FPAs it is only after hybridization that problematic pixels or pixel clusters emerge. Once defective regions have been identified, tailored laser irradiance can be deployed to heat pixels locally. The localization means high anneal temperatures beyond what an entire focal plane assembly can withstand are reached and will be entirely localized to the vicinity of the defect. Because laser beams can be focused to spot sizes much smaller than a pixel, single pixel thermal annealing is possible and allows targeting of only those pixels which exhibit unacceptable levels of noise. This “do no harm” approach ensures functional, acceptable pixels are not degraded or affected by the presence of neighboring defects while annealing.

Most pulsed laser based annealing schemes are not aimed at reducing noise, rather they are integral to the manufacturing process, for example to achieve high temperature dopant activation, minimizing diffusion so dopants stay where the ion implanter places them. While much research has been conducted on how to manufacture and process semiconductor materials with a laser, comparatively little thought has been given to improving device noise characteristics after an FPA has been packaged with readout electronics and before end use.

In FPAS sensor layer defects are not normally detectable until after the sensor layer is hybridized to the readout integrated circuit and tested. At this point the sensor layer cannot be taken off the readout electronics and the entire packaged assembly cannot be heated to temperatures hot enough to promote annealing. Fortunately, the location of problematic pixels or pixel clusters can be identified from characterization and testing and a tightly focused laser can be used to perform a targeted anneal. This approach is innovative from a manufacturing perspective in that it only affects pixels with excessive noise levels and does not operate over the entire array.

Targeted laser annealing to damaged sensors or packaged FPAs prior to use represents an augmentation to state-of-the-art thermal annealing and laser procedures currently done in the manufacturing process. However, laser annealing can be done at any point after manufacturing and before use. For example, if an FPA resides in storage for several months after manufacturing, laser annealing can be used to anneal individual pixels or pixel clusters that may have degraded with time or exposure to radiation.

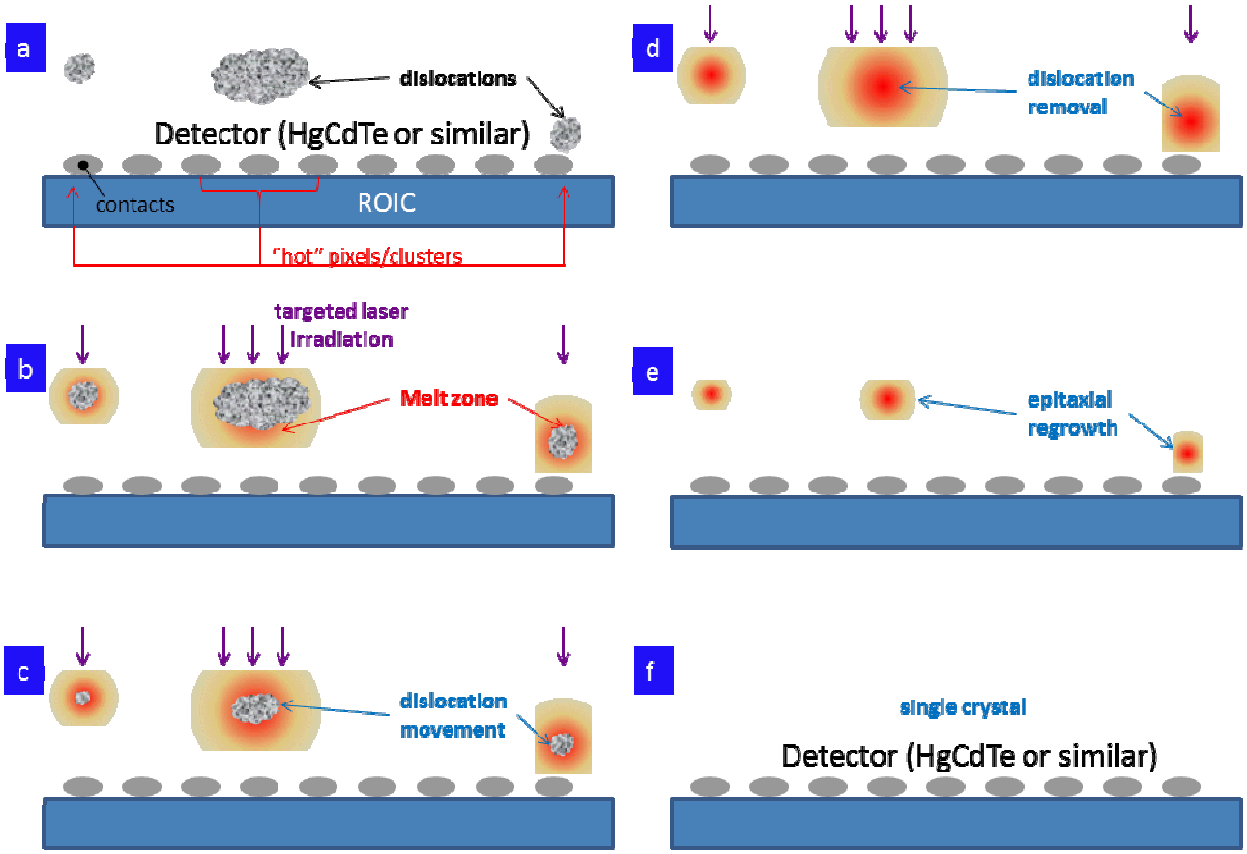

Figure 1. (a) Cross-sectional view of FPA detector and ROIC. Dislocations in the absorbing detector layer lead to increased pixel dark current and "hot" pixels in image acquisition. (b) Targeted laser irradiation heats detector material locally in the vicinity of dislocations. (c) Melted material promotes dislocation movement and lattice relaxation. (d) Dislocation removal occurs after sufficient heat deposit. (e) Surrounding unmelted regions serve as seed layers to epitaxially regrow melted zones. (f) Homogenous single crystal results after anneal.

The process of laser annealing a damaged or defective sensor is outlined in figure 1. Figure 1(a) depicts a cross-sectional view of a detector material bonded to a readout IC (ROIC); electrical contact bumps are shown. Dislocations are illustrated in the detector optical absorption region and appear over both isolated pixels and pixel cluster readouts. Interrogating the ROIC under a dark condition will reveal the location of absorbing layer dislocations due to the presence of increased pixel dark counts. With the coordinates registered for all noisy pixels, targeted laser irradiation can be directed to only those pixels with dislocations or defects, figure 1(b). The laser irradiation is intense enough to locally warm or melt the detector material. A melt zone develops around the location of the defect, allowing the material to become soft, promoting dislocation movement and lattice relaxation, figure 1(c). Following a sufficient heat deposition (typically applied in nanoseconds) dislocations will be removed leaving only a locally melted zone, figure 1(d). After pulsed laser irradiation has concluded, regrowth of the melted zone occurs, figure 1(e). The regrowth process is epitaxial because unmelted material regions surrounding the melt zone serve as a seed layer on which the regrowth process is based. The result is a homogeneous single crystal structure, free of dislocations and defects, figure 1(f). Overall detector array performance is improved because processing is confined to dysfunctional pixels only. The annealing process here is similar to that outlined by J. Yan *et. al.* [1], but is unique in that the annealing takes place in the photodiode junction improving electrical performance, rather than on the surface repairing mechanical damage.

2. EXPERIMENTAL RESULTS

A block diagram of our experimental apparatus is shown in figure 2. The annealing laser is a diode pumped passively Q-switched Nd:YAG operating at 1064 nm and producing an 11 ns (FWHM) pulse. Maximum pulse energy is approximately 200 µJ. Output from the laser is routed through a λ/2 plate and a polarizing beamsplitter (PBS) cube to control the pulse energy. A small percentage of the laser power reflecting off the PBS is detected with a photodiode and oscilloscope for confirmation of laser operation during single shot exposures.

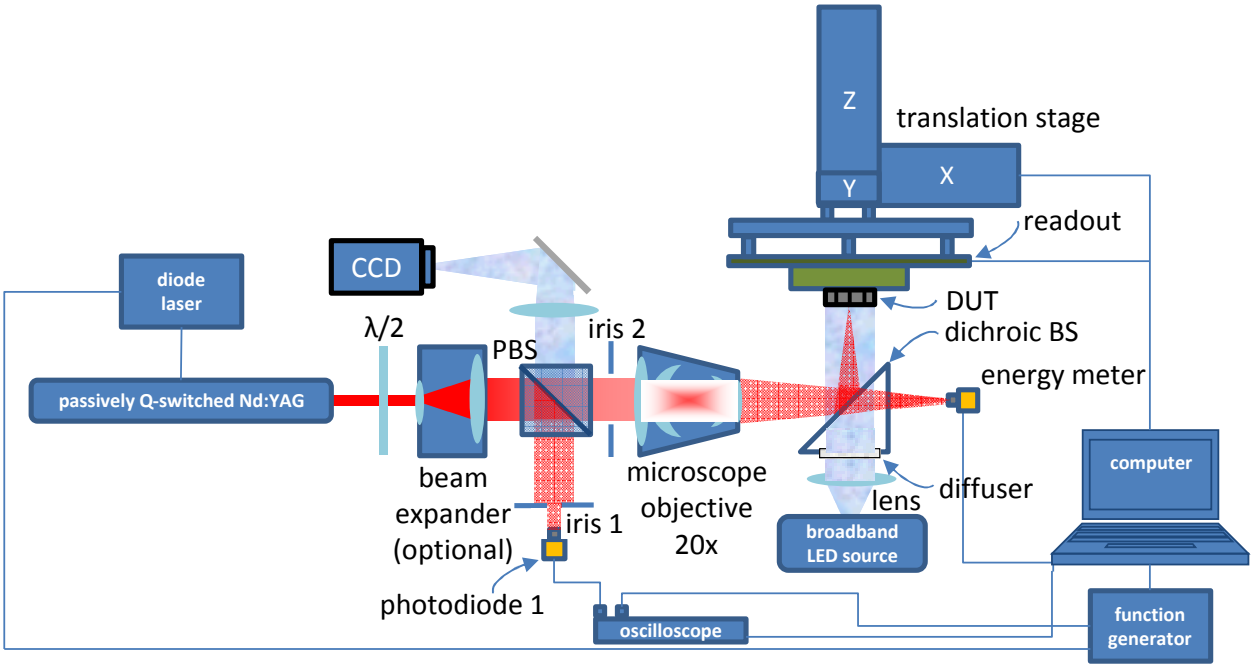

Figure 2. Experimental setup for damaging and laser annealing of Si devices. DUT = device under test, PBS = polarizing beamsplitter.

A 20x NIR microscope objective (NA = 0.28) focuses laser pulses to a spot size of 5 µm (86% encircled energy) at the sample plane. Samples are mounted on a computer controlled XY translation stage with spatial control down to

300 nm. Samples are exposed in the dark to avoid complications of excess carriers due to photo-generation. After a single laser exposure, the photodiode samples undergo a dark IV characterization which is compared to a baseline characterization taken prior to laser exposure. Next the sample is illuminated with a white light LED and the sample surface is imaged with the CCD. After electrical and surface characterization is complete, the laser fluence is increased and the characterization is repeated.

To find the best laser pulse to anneal with, we first electrically damage our photodiode samples with laser fluence above the damage threshold. We find three separate laser damage thresholds associated with the commercial Si photodiodes used in this study (Hamamatsu S2386-18K). Thresholds are summarized in table 1.

Type of damage	**Multi-shot electrical and morphological damage (20 shots @ 1 Hz)**	**Single shot morphological damage, without electrical damage**	**Single shot electrical and morphological damage**
Threshold	1.1 J/cm^2	1.9 J/cm^2	6.7 J/cm^2

Table 1. Three distinct damage thresholds for Si photodiodes. Multi-shot refers to repeated shots in the same spatial location; morphological and electrical damage occur simultaneously.

Here we define electrical damage as a minimum 10x increase in dark current. Morphological and electrical damage are found to occur simultaneously at a fluence of 1.1 J/cm^2 with multiple shots on the same location, see figure 3. This is in contrast to single shot damage thresholds where surface damage always preceded electrical damage. Morphological damage preceding electrical damage has been observed before [2]; however, for CCDs electrical performance can degrade prior to the onset of surface damage [3].

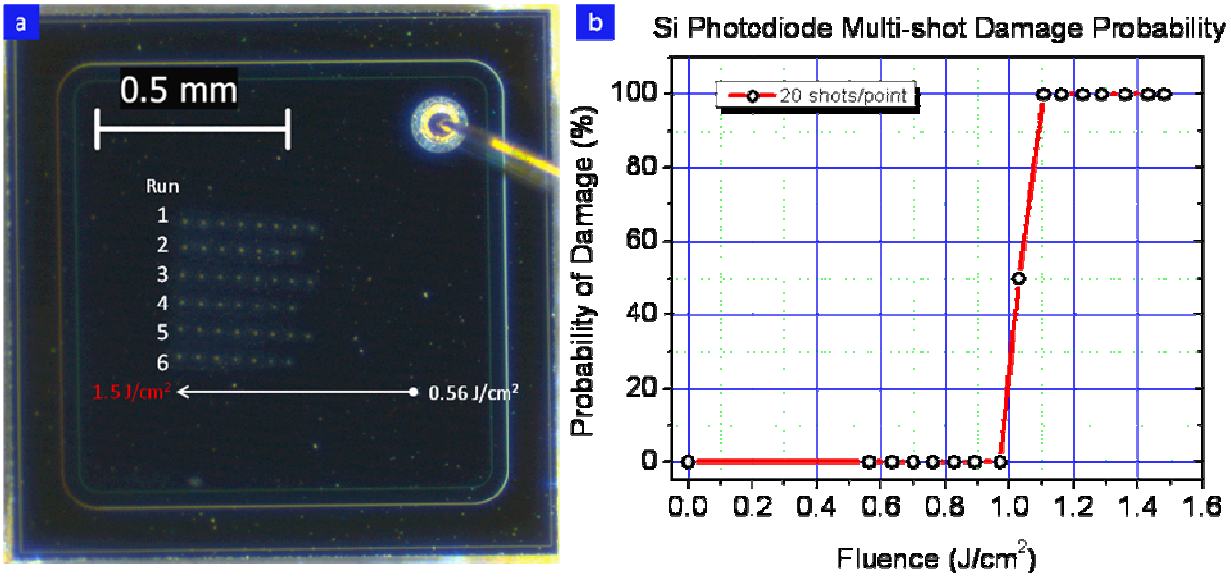

Figure 3. (a) Optical image of photodiode surface after six identical sets of exposures in the fluence range 0.56 to 1.5 J/cm2. Each point was exposed to 20 laser pulses @ 1 Hz. (b) Probability of damage from the fluence data in (a).

For multi-shot investigation the experimental setup is configured to produce one shot every second up to 20 shots. Each shot is at a fixed fluence and at the same location in the active area. With the completion of each 20 shot set,

the surface is interrogated for morphological damage and the dark current measured. Electrical and morphological damage were found to occur coincidently in all cases. After a photodiode was damaged it was exchanged with a new one and the measurement repeated. For four different diodes the electrical and morphological damage was found to be coincident. While the damage was coincident for each, the thresholds were slightly different for each, falling in the range 1.05 to 1.58 J/cm2. The slight variation may be due to diode-to-diode variability or small error in placing the surface of the photodiode exactly at the beam waist. Because electrical and morphological damage are coincident with 20 shot exposures, diode-to-diode variability can be circumvented by using a single diode and monitoring it for surface damage at multiple locations. Six successive identical exposures were performed on a single photodiode active area. Starting from a fluence of 0.56 J/cm^2 and progressing across the active area; the fluence is incremented to 1.5 J/cm^2 in 15 even steps. Each fluence increment consists of 20 laser shots at a 1 Hz repetition rate incident on a new spatial location offset by 75 µm. Morphological (and as a corollary, electrical) damage at all higher fluence levels (≥1.1 J/cm^2) is observed in all six exposure sets while no damage was observed for fluence levels at or below 0.98 J/cm^2. The statistical probability of damage from the six runs is fig. 3(a) is plotted in fig. 3(b). Note the sharp transition at 1.1 J/cm^2, which agrees well with other published values for Si [3].

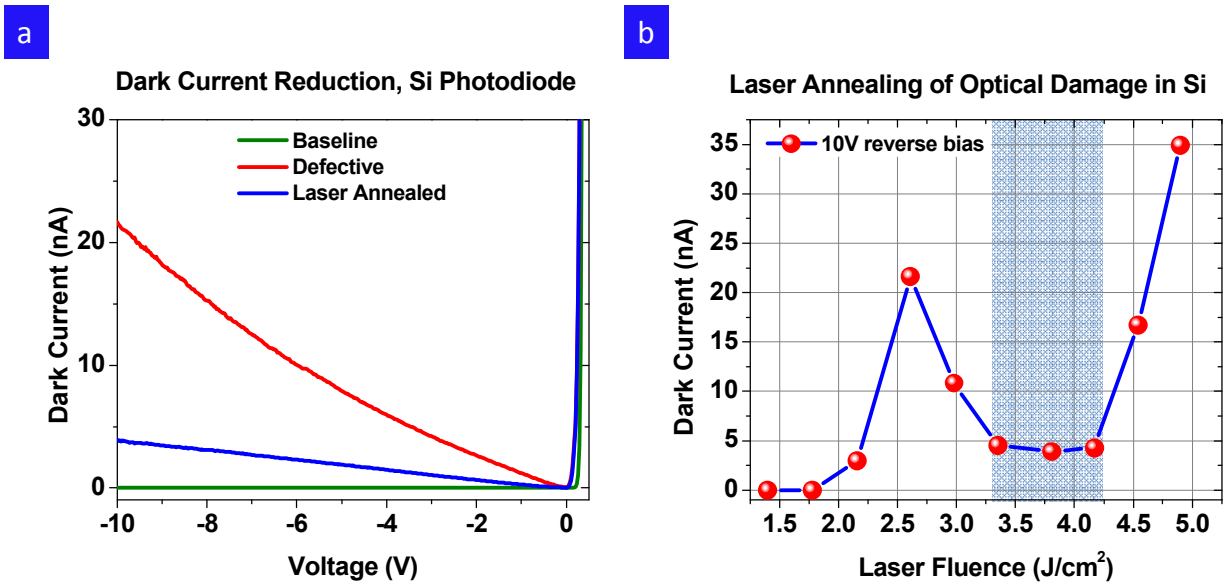

Figure 4. (a) Detector baseline dark current (green line), dark current after damage (red line) and dark current after laser annealing of the damaged site (blue line). Note the substantial reduction (≈5x) in dark current after laser annealing. (b) Dark current after laser exposure, defect creation 2.2 – 2.6 J/cm^2, annealing of created defects 3.25 – 4.25 J/cm^2, irreparable damage >4.25 J/cm^2.

As an example of the power and utility of laser annealing consider the results of figure 4. Our test photodiode is intentionally damage by shining a high-energy Q-switched laser pulse onto the active area with a fluence level above the damage threshold. In this instance the damage threshold is different than the values reported in table 1. This is because it is a ramped fluence multi-shot exposure. That is, each successive laser pulse is of a greater fluence than the preceding pulse. The pulse fluence is continually increased and after each shot the dark current is measured. In this scenario, electrical damage begins at 2.20 J/cm^2, see fig. 4(b). At greater fluence, the dark current continues to increase until 2.6 J/cm^2 after which the dark current begins to decrease. Figure 4(b, shaded region) shows the laser fluence window over which laser annealing takes place and lowers the detector dark current, approximately 3.25 – 4.25 J/cm^2 for a 10 ns, 1064 nm laser pulse. It is, however, important to emphasize that the laser annealing fluence window is device specific; for different detector materials and defects the annealing fluence and laser pulse parameters will change. For fluence in excess of 4.25 J/cm^2 on our device we find the Si boils violently and material

ejecta is observed on the photodiode surface. Dark currents only increase after this point and the damage is irreparable. All pulses are incident on the same location. Figure 4(a, red line) shows the increase in dark current above the detector baseline, Fig. 4(a, green line) after the 2.60 J/cm^2 exposure. Photodiode operability is partially recovered with the careful application of an annealing laser pulse directed at the damage area, Fig. 4(a, blue line) after a 3.80 J/cm^2 exposure. More than a 5× reduction in dark current is measured at a reverse bias voltage of -10 volts. Moreover, dark current is reduced for all reverse bias voltages, indicating that detector performance has been improved throughout the IV curve.

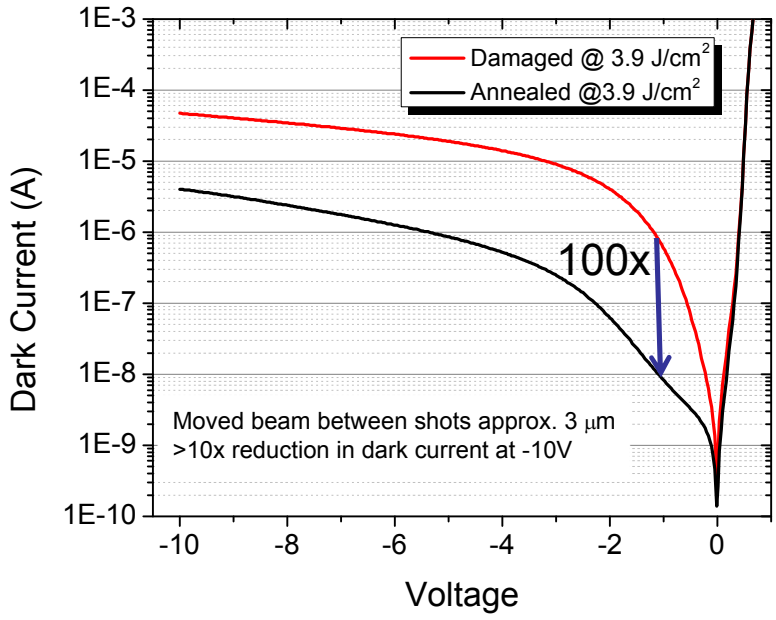

Figure 5. Effect of laser annealing of a damaged detector with a spatial offset between the laser pulse focus and damage site.

With a second series of experiments we consider the effect of spatially offsetting the annealing laser pulse from the damage site. Such an offset allows more undamaged material to be melted and participate in the annealing process. In this case we find an optimum in spatial offset of approximately 3 μm between the damage site and the annealing laser pulse focus. With a spatially offset annealing we were able to achieve a greater than 10x reduction in dark current, see figure 5. Moreover, at low values of reverse bias (≈1 volt) we were able to demonstrate a 100x decrease in dark current. This is particularly important because many FPAs operate at low reverse bias.

To characterize the damage present in Si after dark current degradation has been measured, we perform cross-sectional SEM analysis of the damage site. Figure 6(left) shows that in the case of an un-annealed damage site, subsurface voids are present near the diode junction (700 nm below the surface). Annealing homogenizes the Si surrounding the junction, removing defects and lowering the dark current, figure 6(right). Images presented in figure 6 are only snapshots of a particular cross-section. We performed focused ion beam (FIB) cutting and SEM analysis across the entire damage site. The un-annealed site had two subsurface voids. The annealed site had none.

Optical damage created here could be indicative of adversarial damage; but in this instance serves as a means of creating a region of defects and dislocations approximately the same size as a FPA pixel (≈20 μm). Additionally, the laser damage mimics defects and dislocations present in manufactured IR FPAs. Achieving high yield in the manufacturing of IR FPAs is challenging. These results have been demonstrated on Si, but our future direction is to apply this concept to single pixels in IR materials where FPAs are often plagued with high dark current and noise.

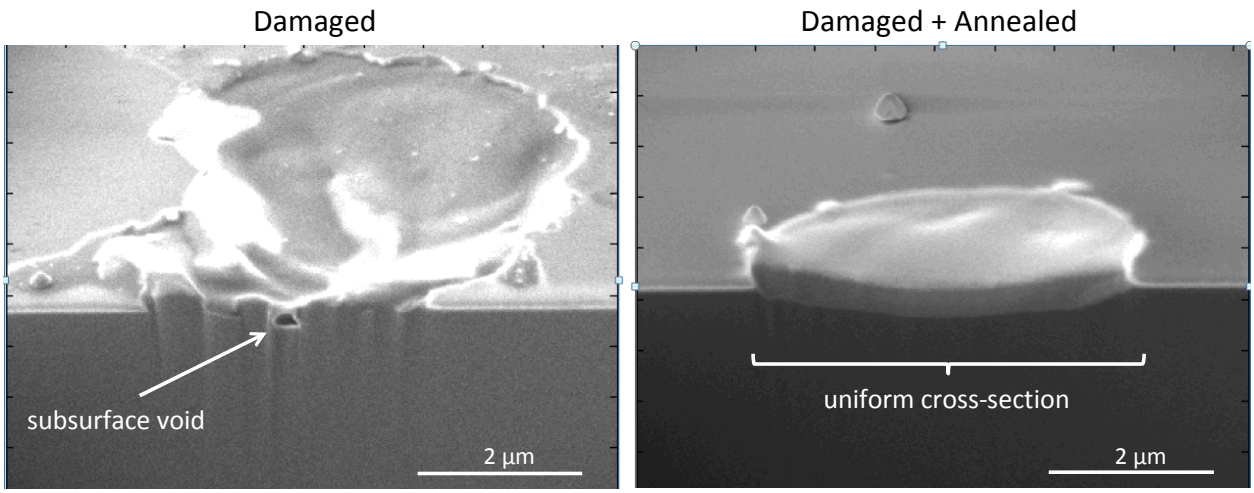

Figure 6. SEM cross-section of damaged and damaged/annealed Si photodiodes. Subsurface voids were found in the case of damage sites that were un-annealed. Homogeneous interfaces were observed between the melt pool and the bulk Si after laser annealing.

Next we consider modification of the optical properties of Si by laser annealing. Specifically, we tune the optical phase acquired in propagation through a single mode waveguide. We fabricate a Mach-Zehnder interferometer out of silicon. One arm of the Mach-Zehnder is shown under magnification in figure 7(a). Broadband coherent light centered at 1550 nm is coupled into the interferometer; output is measured with an optical spectrum analyzer (OSA). The resulting interferogram measured on the OSA is a function of the relative phase difference between each arm of the Mach-Zehnder. A slight change in the optical path length results in a spectral shift of the interference pattern.

Using the same setup detailed in figure 2, we laser anneal small volumes of one arm in the Mach-Zehnder interferometer. To start, a baseline interferogram is measured and recorded with the OSA prior to annealing. Every 10 µm along the propagation axis a single annealing laser pulse is focused onto the waveguide. The pulse fluence varies slightly from shot-to-shot but the mean value is 0.32 J/cm^2 with a standard deviation of 0.0156. After every laser shot the interferogram is re-measured with the OSA and archived. Figure 7(b) shows the evolution of the interferogram for 220 laser shots. After 220 laser shots the phase difference in the interferogram has shifted by a full half wave. This gives an average phase shift of 14.3 mrad per pulse. This level of sensitivity can be used to precisely tune the phase in order to correct for any phase errors that may arise from inhomogeneity in the Si. Furthermore, it is important to note from figure 7(b) that no loss in optical transmission was observed after the 220 laser annealing shots.

3. Summary

In summary, we have shown that precise application of laser pulses can reduce dark current in damaged silicon photodiodes. The greatest reduction in dark current was achieved with slight spatial offsets between a sensor damage site and the focal position of an annealing pulse. We have shown a 100x reduction in dark current from damaged sensors. Additionally, we reported on a means of tuning the propagation phase of light traveling through silicon. Phase control of <15 mrad was demonstrated with laser annealing in silicon waveguides of a Mach-Zehnder interferometer.

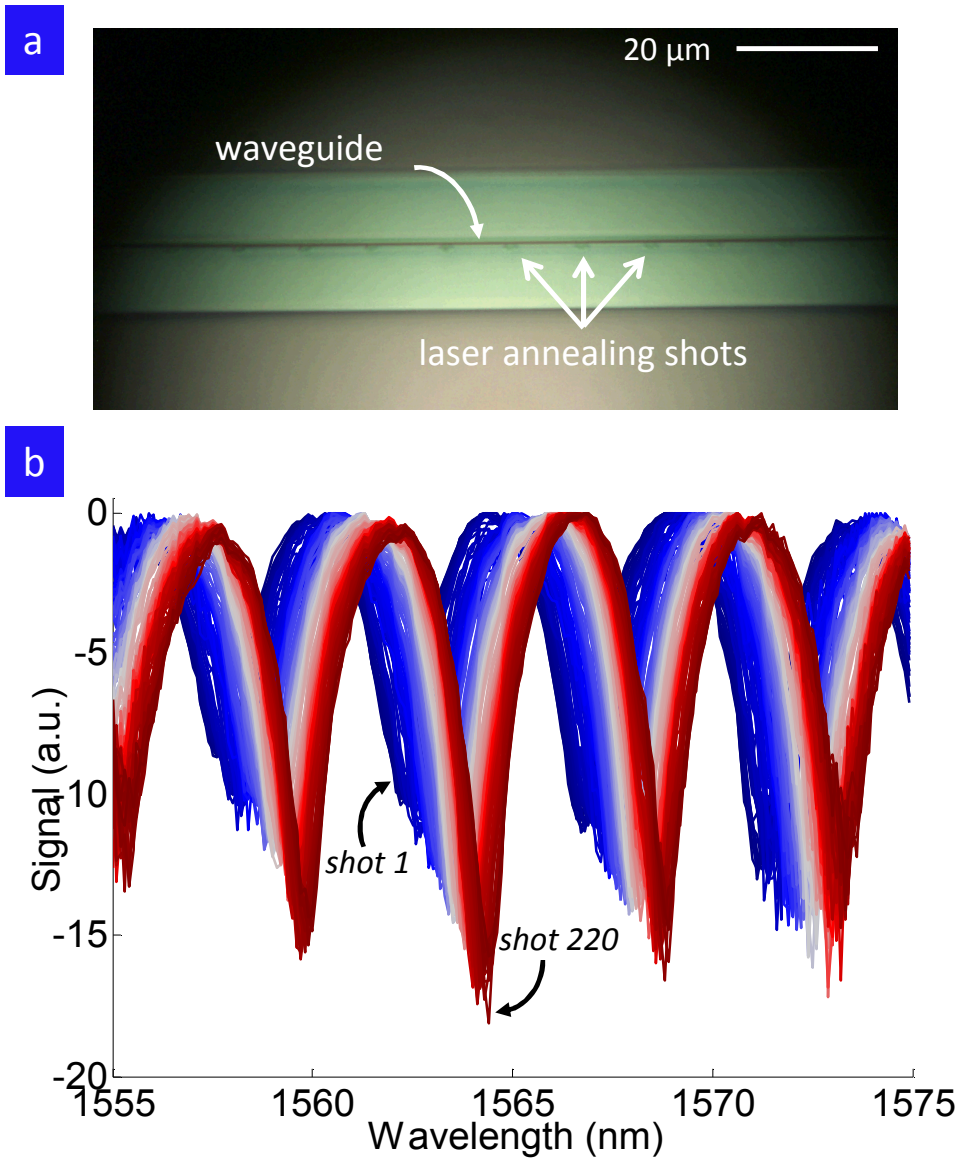

Figure 7. (a) Optical image of a Si waveguide in one arm of a Mach-Zehnder interferometer. Slight melting is seen on the surface of the waveguide, but results in no loss of optical transmission. (b) Series of interferograms measured at the output of the interferometer after each of 220 laser annealing shots; π phase shift is observed.

REFERENCES

[1] J. Yan, *et. al*., "Response of machining-damaged single-crystalline silicon wafers to nanosecond pulsed laser irradiation," *Semi. Sci. & Tech*., **22**, pp. 392-395, (2007).

[2] S. E. Watkins, *et. al*., "Electrical performance of laser damaged silicon photodiodes," *Applied Optics*, **29**, pp. 827-835, (1990).

[3] C. Zhang, *et. al.,*"Laser-induced damage to silicon charge-coupled imaging devices," *Optical Engineering*, **30**, No. 5, pp. 651-657, (1991).